Title

Poplar leaf abscission through induced chlorophyll breakdown by Mg-dechelatase

Author names and affiliations

Hisashi Ito[1], Hideyuki Saito[2], Manabu Fukui[1], Ayumi Tanaka[1], Keita Arakawa[2]

[1]Institute of Low Temperature Science, Hokkaido University, N19 W8, Sapporo 060-0819, Japan

[2]Research Faculty of Agriculture, Hokkaido University, N9 W9, Sapporo 060‐8589, Japan

Corresponding author

Hisashi Ito

Institute of Low Temperature Science, Hokkaido University, N19 W8, Sapporo 060-0819, Japan

Tel; +81-11-706-5469, Fax; +81-11-706-5493, E-mail; ito98@lowtem.hokudai.ac.jp

Keywords

chlorophyll breakdown, defoliation, ethylene, Mg-dechelatase, *Populus*

Abbreviations:

2iP, 2-isopentenyl adenine; DEX, dexamethasone; EF1, elongation factor-1 beta; ERF, ethylene-responsive factor; LHCII, light-harvesting complex of photosystem II; MS, Murashige-Skoog; NAA, naphthaleneacetic acid; RT-PCR, real-time PCR; RubisCO, ribulose-1,5-bisphosphate carboxylase-oxygenase; SGR, Stay-Green

Author contributions

Hisashi Ito: Conceptualization, Investigation, Writing – Original Draft. Hideyuki Saito: Investigation, Writing – Original Draft. Manabu Fukui: Methodology. Ayumi Tanaka: Conceptualization, Funding acquisition. Keita Arakawa: Methodology, Resources.

Funding

This work was supported by the Japan Society for the Promotion of Science, KAKENHI [19K06700 to A. T.].

Abstract

Chlorophyll breakdown is observed during senescence. The first step in chlorophyll breakdown is the removal of central Mg by Mg-dechelatase. This reaction is the rate-limiting step in the chlorophyll breakdown pathway. We evaluated the effect of induced chlorophyll breakdown on abscission through the removal of Mg by Mg-dechelatase. Poplar transformants carrying the dexamethasone-inducible Mg-dechelatase gene were prepared using the Arabidopsis Stay-Green1 cDNA. When leaves were treated with dexamethasone, chlorophyll was degraded, photosynthetic capacity was reduced, and an abscission zone was formed, resulting in leaf abscission. In addition, ethylene, which plays an important role during senescence, was produced in this process. Thus, chlorophyll breakdown induces the phenotype in the same way as commonly observed during leaf senescence. This study suggests a physiological role of chlorophyll breakdown in the leaf abscission of deciduous trees. Furthermore, this study shows that the dexamethasone-inducible gene expression system is an available option for deciduous tree studies.

1. Introduction

The change in the color of leaves signifies the autumn season and is achieved through chlorophyll breakdown. The initial step of chlorophyll breakdown is the removal of central Mg by Mg-dechelatase [1]. The gene encoding Mg-dechelatase is called *Stay-Green* (*SGR*, also known as *Non Yellowing 1*) because it was first identified as the gene responsible for the stay-green phenotype during senescence [2]. *SGR* induction is controlled by light and plant hormones, such as ethylene and jasmonate, at the senescence stage, making it a typical senescence-associated gene [3]. Removing Mg from the chlorophyll molecule results in the formation of pheophytin; thereafter, the phytyl group of pheophytin is removed by hydrolysis, and the tetrapyrrole ring opens for further degradation [4]. SGR catalyzes the rate-limiting step of the chlorophyll breakdown pathway. Chlorophyll levels are low in SGR-overexpressing plants, whereas chlorophyll breakdown is markedly suppressed in SGR-deficient *Arabidopsis thaliana* mutants [1, 5]. SGR studies are essential to investigate the regulation of chlorophyll breakdown.

It is crucial to salvage a large portion of nitrogen contained in the chloroplast, owing to the proteins of the chlorophyll-protein complex such as light-harvesting complex of the photosystem II (LHCII), during senescence [6]. Chlorophyll breakdown is essential to salvage nitrogen derived from the degraded protein because the chlorophyll-protein complex is tolerant to protease attack. Hence, chlorophyll should be removed before proteolysis [7]. Furthermore, free chlorophyll produces reactive oxygen species that can damage cells and interfere with nutrient recovery [8]. Thus, chlorophyll must be degraded during senescence.

Due to the reduction in photosynthetic capacity under low temperature, deciduous trees abscise their leaves in autumn. If leaves are left unshed during the winter, the weight of the snow may damage branches [9]. In addition, the unshed leaves block the light for the new shoots that will emerge in spring. Defoliation is caused by the formation of an abscission zone at the leaf base. The study on the formation of an abscission zone has advanced owing to the use of mutants of Arabidopsis [10]. Arabidopsis enables a favorable genetic approach, but is not deciduous. Therefore, it is necessary to investigate trees to elucidate their underlying mechanisms. *Populus* (poplar) is a deciduous tree, and its deciduous mechanism has been extensively studied [11]. Ethylene promotes the formation of the abscission zone. Auxin shows a negative impact on ethylene function in the abscission zone. Auxin depletion makes cells more sensitive to ethylene, which promotes abscission zone formation [10, 12]. Factors involved in abscission zone formation in poplar are generally the same as those in Arabidopsis [9].

Using Arabidopsis transformants in which *AtSGR* can be induced by dexamethasone treatment, we previously reported that chlorophyll breakdown leads to jasmonate synthesis and induces senescence-related genes [13]. Chlorophyll breakdown results from senescence but also promotes jasmonate production. In this study, we investigated how chlorophyll breakdown influences defoliation, a phenomenon that is important for generating new shoots, in poplar.

2. Materials and methods

2.1 Plant growth conditions and transformation

Poplar was cultured and transformed as described previously [14, 15] with minor modifications. Briefly, *Populus alba* × *Populus tremula* was grown on a half-strength Murashige-Skoog (MS) medium containing 5 % (w/v) sucrose, 1 mM MES-NaOH (pH 5.8), and 6 % (w/v) agar under sterile conditions. The Arabidopsis *SGR1* (*AtSGR1*) gene (AT4G22920) was cloned into a DEX-inducible vector [16, 17] as described previously [1]. For poplar transformation, stems were cut into 1 cm pieces and incubated on half-strength MS medium containing 3 % (w/v) sucrose, 1 mM MES-NaOH (pH 5.8), 10 µM naphthaleneacetic acid (NAA), 5 µM 2-isopentenyladenine (2iP), and 6 % (w/v) agar for 2 d. Cultured *Agrobacterium tumefaciens* (strain GV3101) carrying the vector was resuspended (OD_{600} = 0.5) in MS medium containing 20 µM acetosyringone and incubated for 1 h. Thereafter, the stems were incubated with an Agrobacterium suspension for 1 h with shaking and then incubated for 2 d on agar medium supplemented with a plant hormone under dark conditions. The stems were then washed with MS medium containing 100 µg mL^{-1} carbenicillin and 50 µg mL^{-1} cefotaxime. For callus induction, stems were incubated on MS medium containing 5 % (w/v) sucrose, 1 mM MES-NaOH (pH 5.8), 6 % (w/v) agar, 50 µg mL^{-1} kanamycin, 500 µg mL^{-1} carbenicillin, 250 µg mL^{-1} cefotaxime, 10

μM NAA, and 5 μM 2iP for 2 w under dark conditions. Shoots were generated by incubation on MS medium containing 5 % (w/v) sucrose, 1 mM MES-NaOH (pH 5.8), 6 % (w/v) agar, 50 μg mL^{-1} kanamycin, 500 μg mL^{-1} carbenicillin, 250 μg mL^{-1} cefotaxime, and 0.1 μM thidiazuron for 2 w under 16 h light and 8 h dark conditions. Following root initiation, the plants were transferred to fertilized soil and grown at 24 °C under continuous light (100 μmol photons m^{-2} s^{-1}). Plants were grown in soil for approximately 2 months, and once they reached approximately 30 cm in height, they were used for the experiments. For *AtSGR1* induction, plants were sprayed with 10 μM DEX, supplemented with 0.01 % Silwet L-77. The mock treatment consisted of Silwet L-77 solution.

2.2 Histology

Samples were fixed in an aqueous solution (formaldehyde: acetic acid: 70 % ethanol=1:1:18), dehydrated in a tertiary butanol series and embedded in paraffin (Tissueprep, Fisher Scientific). Sections were obtained using a microtome (Leica RM2135 microtome, Leica), heat-fixed to a glass slide, then stained with 0.1 %Toluidine Blue.

2.3 Chlorophyll and protein analysis

Fully and almost fully expanded leaves were used for the analysis. Chlorophyll levels were measured using SPAD-502Plus (Konica Minolta). For protein analysis, leaf disks (1 cm^2) were frozen in liquid nitrogen and disrupted by shaking them with zirconia beads. Proteins were extracted from the leaf powder in 400 μL of protein extraction buffer (125 mM Tris-HCl, pH 6.8, 2 % [w/v] sodium dodecyl sulfate, 5 % [w/v] sucrose, and 2.5 % [v/v] 2-mercaptoethanol). After centrifugation (20,000 × *g*, 5 min), the supernatant was subjected to sodium dodecyl sulfate-polyacrylamide gel electrophoresis. The electrophoresed proteins were transferred onto a polyvinylidene difluoride membrane for immunoblot analysis, as described previously [5]. For the immunoblot analysis of CP43 and Lhca1, 2 μL of the supernatant was subjected to electrophoresis. For the immunoblot analysis of PsaA/B, D1, and Lhcb1, 2 μL of the 10 times diluted supernatant was subjected to electrophoresis. When D1 was analyzed, 6 M urea was used in the gel. The anti-CP1 (PsaA/PsaB) and anti-CP43 antibodies were prepared as previously described [18]. We purchased antibodies against D1 (AS11 1786), Lhca1 (AS01 005), and Lhcb1 (AS01 004) proteins from Agrisera. The primary antibody was diluted with immunoreaction enhancer solution (Can Get Signal; Toyobo). Anti-rabbit IgG conjugated to horseradish peroxidase was used as the secondary antibody. Horseradish peroxidase activity was visualized using the Western Lightning Plus-ECL Chemiluminescence Detection Kit (PerkinElmer).

2.4 RNA isolation and quantitative real-time polymerase chain reaction (qRT-PCR)

RNA was extracted from leaf tissues using the Plant RNA Purification Reagent (Invitrogen). The cDNA was synthesized using a PrimeScriptRT Reagent Kit with gDNA eraser (Takara). The qRT-PCR analysis was performed using SsoAdvanced Universal SYBR

Green Supermix (Bio-Rad) and MyiQ2 (Bio-Rad). *Elongation factor1-beta* (*EF1*) (Potri_009G018600) was amplified using the primer sets: 5`-AAC CTG GTC GTG ATT TCC CT-3` and 5`-ATC ACC AGC AGC CTC CTT G-3`, and used as a reference gene [19]. *AtSGR1* was amplified using the primer sets: 5`-CAT TGT CAC ATA AGC GGT GG-3` and 5`-AGT TCC CAT CTC CAT GCA C-3`. *Ethylene-responsive factor12* (*ERF12*) (Potri.011G061700) was amplified using the primer sets: 5`-CAG ATC CAT GAG CTC CCC TTT-3` and 5`-GCC TGA AGT GTT GAT TTG GCT T-3`. Among the ethylene-responsive factors, *ERF12* was chosen because it is induced during the natural senescence stage [19].

2.5 Analysis of gas exchange

Photosynthetic capacity was measured just before and after 3 d and 8 d of DEX treatment. Light saturated CO_2 assimilation rate was assessed by the gas-exchange method with infrared gas analyzer for CO_2 and H_2O. Simultaneous measurements of CO_2 assimilation rate and transpiration rate were conducted by using a portable photosynthesis measurement system with a 2 X 3 cm broad leaf chamber and LED light source (LI6400, LI-COR, Lincoln). Photosynthetic photon flux density was controlled at 1500 µmol photons m^{-2} s^{-1}. The inlet gas CO_2 concentration to the chamber was 400 µmol mol^{-1}. The air temperature and leaf-to-air water vapor pressure deficit in the gas exchange chamber were controlled at 25 °C and approximately 0.7–1.0 kPa, respectively.

2.6 Measurement of ethylene concentration

Leaves were treated with DEX and incubated for 1 d, trimmed to approximately 400 mg, and incubated in 20 mL vials under continuous light conditions for 1 d. Next, 0.5 mL of gas was collected using a gas-tight syringe, measured using a gas chromatograph (GC-2014; Shimadzu) fitted with a column (Porapak-N 50-80, GL Sciences) and flame ionization detector. The gas was analyzed using Chromatopac C-R8A (Shimadzu). Nitrogen was used as the carrier gas. The injector, column, and detector temperatures were adjusted to 120, 100, and 120 °C, respectively. Ethylene gas (GL Sciences) was used as a standard to quantify the detected ethylene.

3. Results

3.1 Chlorophyll breakdown and defoliation after *SGR* induction

We investigated the degradation of chlorophyll by SGR following DEX treatment. We used Arabidopsis *SGR1* (*AtSGR1*) instead of endogenous *SGR* because the genome of *Populus alba* x *Populus tremula* [20] had not been revealed when we prepared the transformed poplar. Furthermore, a homogeneous gene could induce gene suppression. Introducing a heterogenous gene will have less possibility of causing this problem [21].

Hence, we used *AtSGR1*. *AtSGR1* was introduced into poplar under the control of the pOp6 promoter and synthetic transcription factor LhGR. LhGR is constructed by fusing the ligand-binding domain of a rat glucocorticoid receptor with the synthetic transcription factor LhG4. After treatment with DEX, LhGR enters the cell nucleus and activates the pOp promoter [16, 17]. Two independent transformants (lines 1 and 2) were treated with DEX. The chlorophyll content was determined using SPAD. SPAD values were normalized on day zero for each sample. DEX-treated leaves turned yellow (Fig. 1A), decreasing chlorophyll levels (Fig. 2). Mock-treated leaves did not change color. Although both transformants showed yellowing, Line 1 showed a markedly decrease in chlorophyll levels compared with that in Line 2 (Fig. 2).

The expression of *AtSGR1* mRNA was examined to confirm that the decrease in chlorophyll levels was due to AtSGR1 catalysis. The mRNA levels were normalized to *EF1* expression. After 2 d of DEX treatment, *AtSGR1* mRNA levels increased and were almost the same after 4 d in Line 1 (Fig. 3). In Line 2, the mRNA levels also increased; however, the levels were lower than those in Line 1. Mock-treated leaves did not exhibit an increase in *AtSGR1* mRNA levels. These observations suggest that chlorophyll was degraded by the induced *AtSGR1,* and the rates of chlorophyll level decrease are likely to correlate with *AtSGR1* levels.

3.2 Decrease of photosynthetic activity and degradation of chloroplast protein through chlorophyll breakdown

Reduction in photosynthetic activity is a marker of senescence. We investigated whether DEX-induced chlorophyll breakdown reduces photosynthetic activity, similar to natural senescence. The leaves of each line were examined. Line 1 showed a decrease in photosynthesis rates on day three and a further decrease on day eight (Fig. 4). Line 2 also showed a decrease in photosynthetic rate on day three of DEX treatment and a greater decrease on day eight, although less pronounced than that in Line 1. The untreated leaves showed no decrease in photosynthetic rate until day eight. These results indicate that similar to natural senescence, chlorophyll breakdown induced by DEX treatment results in a decrease in photosynthetic capacity.

The levels of the core complexes and light-harvesting complexes of the photosystem were evaluated using immunoblot analysis (Fig. 5). The levels of the core complexes of photosystem I (PsaA/B) and photosystem II (D1 and CP43) decreased after DEX treatment in line 1. The levels of the light-harvesting complexes of photosystem I (Lhca1) and photosystem II (Lhcb1) also decreased in the DEX-treated plants. Mock-treated plants did not show any decrease in the levels of these proteins. Though the changes in protein levels were less significant, line 2 also showed that the levels of PsaA/B, CP43, and Lhcb1 decreased after DEX treatment. These observations suggest that chlorophyll *a* breakdown through SGR expression resulted in a decrease in the levels of chlorophyll-protein complexes.

Although the decrease in photosynthetic capacity may be partially attributed to the reduction in the levels of chlorophyll-protein complexes, the significant decrease in photosynthetic capacity on day three (Fig. 4) cannot be explained by the decrease in photosystem protein levels. The molecular mechanism of the decrease in the net photosynthesis rate needs to be elucidated.

3.3 Abscission zone formation and ethylene production through chlorophyll breakdown

In the leaves in which *SGR* was induced by DEX treatment, the yellowing leaves eventually fell off in Line 1 (Fig. 1A). At this point, an abscission zone was observed (Fig. 1B). The exact timing of abscission zone formation could not be identified by observing the petioles. Neither defoliation nor abscission zones were observed in mock-treated leaves.

We examined whether ethylene is produced when chlorophyll breakdown is induced by DEX treatment since ethylene is involved in abscission zone formation. DEX was administered to the leaves, and leaves were collected the next day and placed in glass containers. The amount of ethylene in the glass containers was measured the following day. The amount was markedly higher than that in the untreated leaves (Fig. 6). These results suggest that ethylene was produced by chlorophyll breakdown.

ERFs are components of the ethylene signal transduction pathway. To examine whether the leaves in which chlorophyll breakdown was induced on DEX treatment were responsive to ethylene, we determined the expression of *ERF12* mRNA. An increase in mRNA levels was observed on the second day of DEX treatment when compared with that in untreated leaves (Line 1). Line 2 exhibited increased *ERF12* mRNA levels, although the difference was not statistically significant. *ERF12* expression suggested that chlorophyll breakdown by DEX treatment activates the ethylene signal transduction pathway. Abscission zone formation also suggests the activation of the ethylene signal transduction pathway in DEX-treated leaves.

4. Discussion

4.1 Application of dexamethasone-inducible gene expression system to poplar study

Artificial induction of transgene expression in plants allows us to deregulate gene expression levels at specific stages and specific tissues of interest. Dexamethasone is a widely used chemical for inducible gene expression systems in herbaceous plants [22]. However, application of this system to poplar study is limiting [23]. In this study, we successfully induced the *AtSGR1* expression and chlorophyll degradation. This study shows that the dexamethasone-inducible gene expression system is available and useful in poplar research.

4.2 Physiological response of poplar leaves to the induced chlorophyll breakdown

Chlorophyll breakdown is considered as one of the most remarkable phenomena associated with senescence. It induces collapse of thylakoid membrane structure in chloroplasts [24]. This dynamic change in organelles may impact the physiological conditions of the cell. To examine the effect of chlorophyll breakdown on tree leaf senescence, we investigated transformed poplars in which chlorophyll breakdown can be induced by DEX treatment. Constitutive SGR-overexpressing plants show yellow seedlings and growth defects [1]. Therefore, inducible gene expression systems are useful in SGR studies. Under field conditions, poplars degrade chlorophyll, and their photosynthetic capacity decreases when the temperature drops in autumn. Nitrogen levels also decrease through remobilization [25, 26]. When chlorophyll breakdown was artificially induced in mature leaves, photosynthetic activity was reduced (Fig. 4), and chlorophyll-protein complexes were also degraded (Fig. 5). These observations indicated that leaves respond to natural senescence and artificially induced chlorophyll breakdown similarly. The primary physiological significance of leaf senescence is the salvage of nutrients. It remains to be determined whether nitrogen derived from degraded chlorophyll-protein complexes is remobilized and reused.

4.3 Chlorophyll breakdown and ethylene production

In the present study, ethylene was produced when chlorophyll breakdown was induced (Fig. 6). It was also observed that the leaves formed an abscission zone and dropped after the chlorophyll levels were significantly decreased (Fig. 1). Defoliation is induced by ethylene production [9]. Therefore, defoliation may be achieved by the ethylene produced through the induction of chlorophyll breakdown. However, the direct implications of chlorophyll breakdown on ethylene production cannot be speculated. Ethylene is synthesized from S-adenosylmethionine via a two-step reaction involving 1-aminocyclopropane-1-carboxylic synthase and 1-aminocyclopropane-1-carboxylic oxidase [27]. The 1-aminocyclopropane-1-carboxylic synthase reaction is thought to be the major regulatory step in ethylene biosynthesis; however, there are many other regulatory sites. It has still not been determined as to which regulatory step is activated in the transformed poplar.

Chlorophyll is degraded in the chloroplasts, whereas ethylene biosynthesis occurs in the cytoplasm. Since chlorophyll breakdown and ethylene biosynthesis occur at different sites, it is unlikely that chlorophyll breakdown directly activates the enzymes involved in ethylene biosynthesis. Chlorophyll catabolites observed in the pheophorbide *a*/phyllobilin pathway are supposed to have physiological effects on metabolism in the plant cells. They produce reactive oxygen species when they absorb light [8]. Pheophorbide *a* may act as a signal that triggers a specific jasmonate response at a defined time [28]. A significant amount of phyllobilin that accumulated in response to insect or fungal attacks can have a physiological role in protection [29]. Among these possible effects of chlorophyll catabolite

accumulation, the production of reactive oxygen species is the most likely trigger of ethylene biosynthesis because stress conditions generally induce ethylene production. In field-grown poplar, approximately half of the chlorophyll was observed to be degraded in 10 days [25]. The rate of chlorophyll breakdown observed in this study is not remarkably different from that observed under natural conditions. If chlorophyll catabolites caused oxidative stress and induced ethylene biosynthesis in this study, the same process may be occurring under natural conditions. Abscission is also observed when leaves are incubated under dark conditions [11]. This may be because of starvation-induced senescence [30]. Chlorophyll breakdown also causes starvation owing to a lack of photosynthesis, and this stress can be related to ethylene biosynthesis. The relationship between chlorophyll breakdown and ethylene biosynthesis remains an important but unanswered question.

5. Conclusion

This study showed that procedures used for herbaceous model plants, such as Arabidopsis, can also be used for deciduous trees. This study aimed to elucidate the physiological significance of chlorophyll breakdown in deciduous tree leaves. The leaves used in this study were young and grown under optimal growth conditions, thus differing from the natural autumn leaves that are subjected to lower temperatures and a shorter duration of daylight. We used these leaves to determine the sole effect of chlorophyll breakdown on defoliation. Using transformed poplar for the investigation of defoliation, we found that chlorophyll breakdown is correlated with ethylene production and the formation of an abscission zone, resulting in defoliation. Leaf yellowing and leaf drop create an autumnal landscape. SGR is suggested to play an important role in these events. How chlorophyll breakdown affects cellular function needs to be elucidated at the molecular level.

Acknowledgments

We thank Prof. Ryouichi Tanaka of Hokkaido University for the helpful discussions.

Figure legends

Fig.1. Leaf yellowing and abscission zone formation

(A) Images of plants. Mock- and DEX-treated plants were grown under continuous light. The defoliating leaves are pointed with the blue arrows on day eight. (B) Images of petioles. The petioles of mock- and DEX-treated plants were observed using a microscope

after 7 d of DEX treatment. Right panels show a toluidine blue-stained longitudinal section. The abscission zone is pointed with the blue arrow in the DEX-treated plants.

Fig. 2. Changes in chlorophyll levels

Chlorophyll levels were measured on the same leaves every 2 d for 8 d using SPAD. The levels were normalized from the day 0 value to 1. The bars represent the standard deviations of three biological replicates derived from the independent lines. *$p < 0.05$, **$p < 0.01$, unpaired *t*-test.

Fig. 3. Changes in CO_2 assimilation rates

CO_2 assimilation rates were examined after 0, 3, and 8 d of mock or DEX treatment of the same leaves. The bars represent the standard deviations of three biological replicates derived from the independent leaves. *$p < 0.05$, **$p < 0.01$, unpaired *t*-test.

Fig. 4. Expression of inducible *SGR* and ethylene response factor genes

RNA was extracted from three independent plants of each transformant after mock or DEX treatment on days 0, 2, and 4. The mRNA levels were examined by quantitative RT-PCR using specific primer sets. The mRNA levels in each sample were normalized to those of *EF-1*. The bars represent the standard deviations of three biological replicates derived from the independent lines. *$p < 0.05$, **$p < 0.01$, unpaired *t*-test.

Fig. 5. Changes in protein levels involved in photosynthesis

Proteins were extracted from the leaf disks of mock-and DEX-treated leaves. The applied samples were normalized to the leaf area. Each protein was detected using specific antibodies. A dilution series was prepared with mock 0 day protein.

Fig. 6. Ethylene production after *SGR* induction

Mock- or DEX-treated plants were incubated for 1 d before sampling. The leaves were cut and incubated in vials for 1 d under continuous light conditions. The amount of ethylene accumulated in the vials was measured by gas chromatography. The bars represent standard deviations of three biological replicates. **$p < 0.01$, unpaired *t*-test.

References

[1] Y. Shimoda, H. Ito, A. Tanaka, Arabidopsis STAY-GREEN, Mendel's green cotyledon gene, encodes magnesium-dechelatase, Plant Cell, 28 (2016) 2147-2160.
[2] S.Y. Park, J.W. Yu, J.S. Park, J. Li, S.C. Yoo, N.Y. Lee, S.K. Lee, S.W. Jeong, H.S. Seo, H.J. Koh, J.S. Jeon, Y.I. Park, N.C. Paek, The senescence-induced staygreen protein regulates chlorophyll degradation, Plant Cell, 19 (2007) 1649-1664.

[3] B. Kuai, J. Chen, S. Hörtensteiner, The biochemistry and molecular biology of chlorophyll breakdown, J. Exp. Bot., 69 (2018) 751-767.
[4] B. Kräutler, Breakdown of chlorophyll in higher plants—Phyllobilins as abundant, yet hardly visible signs of ripening, senescence, and cell death, Angew. Chem., Int. Ed., 55 (2016) 4882-4907.
[5] Y. Chen, W. Yamori, A. Tanaka, R. Tanaka, H. Ito, Degradation of the photosystem II core complex is independent of chlorophyll degradation mediated by Stay-Green Mg2+ dechelatase in Arabidopsis, Plant Sci., 307 (2021) 110902.
[6] A. Makino, H. Sakuma, E. Sudo, T. Mae, Differences between Maize and Rice in N-use Efficiency for Photosynthesis and Protein Allocation, Plant Cell Physiol., 44 (2003) 952-956.
[7] S. Hörtensteiner, U. Feller, Nitrogen metabolism and remobilization during senescence, J. Exp. Bot., 53 (2002) 927-937.
[8] S. Hörtensteiner, Chlorophyll degradation during senescence, Annu. Rev. Plant Biol., 57 (2006) 55-77.
[9] O.R. Patharkar, J.C. Walker, Advances in abscission signaling, J. Exp. Bot., 69 (2018) 733-740.
[10] S. Meir, S. Philosoph-Hadas, J. Riov, M.L. Tucker, S.E. Patterson, J.A. Roberts, Re-evaluation of the ethylene-dependent and -independent pathways in the regulation of floral and organ abscission, J. Exp. Bot., 70 (2019) 1461-1467.
[11] X. Jin, J. Zimmermann, A. Polle, U. Fischer, Auxin is a long-range signal that acts independently of ethylene signaling on leaf abscission in Populus, Front. Plant Sci., 6 (2015).
[12] J.A. Roberts, K.A. Elliott, Z.H. Gonzalez-Carranza, Abscission, Dehiscence, and Other Cell Separation Processes, Annu. Rev. Plant Biol., 53 (2002) 131-158.
[13] K. Ono, M. Kimura, H. Matsuura, A. Tanaka, H. Ito, Jasmonate production through chlorophyll a degradation by Stay-Green in Arabidopsis thaliana, J. Plant Physiol., 238 (2019) 53-62.
[14] C. Benedict, J.S. Skinner, R. Meng, Y. Chang, R. Bhalerao, N.P.A. Huner, C.E. Finn, T.H.H. Chen, V. Hurry, The CBF1-dependent low temperature signalling pathway, regulon and increase in freeze tolerance are conserved in Populus spp, Plant Cell Environ., 29 (2006) 1259-1272.
[15] O. Nilsson, T. Aldén, F. Sitbon, C.H. Anthony Little, V. Chalupa, G. Sandberg, O. Olsson, Spatial pattern of cauliflower mosaic virus 35S promoter-luciferase expression in transgenic hybrid aspen trees monitored by enzymatic assay and non-destructive imaging, Transgenic Res., 1 (1992) 209-220.
[16] A. Wielopolska, H. Townley, I. Moore, P. Waterhouse, C. Helliwell, A high-throughput inducible RNAi vector for plants, Plant Biotechnol. J., 3 (2005) 583-590.
[17] J. Craft, M. Samalova, C. Baroux, H. Townley, A. Martinez, I. Jepson, M. Tsiantis, I. Moore, New pOp/LhG4 vectors for stringent glucocorticoid-dependent transgene expression in Arabidopsis, Plant J., 41 (2005) 899-918.
[18] A. Tanaka, Y. Yamamoto, H. Tsuji, Formation of chlorophyll-protein complexes during greening 2. Redistribution of chlorophyll among apoproteins, Plant Cell Physiol., 32 (1991) 195-204.
[19] H. Lu, M.I. Gordon, V. Amarasinghe, S.H. Strauss, Extensive transcriptome changes during seasonal leaf senescence in field-grown black cottonwood (Populus trichocarpa Nisqually-1), Sci. Rep., 10 (2020) 6581.
[20] D. Qiu, S. Bai, J. Ma, L. Zhang, F. Shao, K. Zhang, Y. Yang, T. Sun, J. Huang, Y. Zhou, D.W. Galbraith, Z. Wang, G. Sun, The genome of Populus alba x Populus tremula var. glandulosa clone 84K, DNA Res, 26 (2019) 423-431.
[21] M.A. Matzke, J.A. Birchler, RNAi-mediated pathways in the nucleus, Nature reviews. Genetics, 6 (2005) 24-35.

[22] L. Borghi, Inducible Gene Expression Systems for Plants, in: L. Hennig, C. Köhler (Eds.) Plant Developmental Biology, Humana Press, 2010, pp. 65-75.
[23] M. Yamaguchi, N. Goué, H. Igarashi, M. Ohtani, Y. Nakano, J.C. Mortimer, N. Nishikubo, M. Kubo, Y. Katayama, K. Kakegawa, P. Dupree, T. Demura, VASCULAR-RELATED NAC-DOMAIN6 and VASCULAR-RELATED NAC-DOMAIN7 Effectively Induce Transdifferentiation into Xylem Vessel Elements under Control of an Induction System, Plant Physiol., 153 (2010) 906-914.
[24] T. Sato, Y. Shimoda, K. Matsuda, A. Tanaka, H. Ito, Mg-dechelation of chlorophyll a by Stay-Green activates chlorophyll b degradation through expressing Non-Yellow Coloring 1 in Arabidopsis thaliana, J. Plant Physiol., 222 (2018) 94-102.
[25] J. Keskitalo, G. Bergquist, P. Gardeström, S. Jansson, A Cellular Timetable of Autumn Senescence, Plant Physiol., 139 (2005) 1635-1648.
[26] T.W. Jurik, SEASONAL PATTERNS OF LEAF PHOTOSYNTHETIC CAPACITY IN SUCCESSIONAL NORTHERN HARDWOOD TREE SPECIES, Am. J. Bot., 73 (1986) 131-138.
[27] J. Pattyn, J. Vaughan‐Hirsch, B. Van de Poel, The regulation of ethylene biosynthesis: a complex multilevel control circuitry, New Phytol., 229 (2020) 770-782.
[28] S. Aubry, N. Fankhauser, S. Ovinnikov, A. Pružinská, M. Stirnemann, K. Zienkiewicz, C. Herrfurth, I. Feussner, S. Hörtensteiner, Pheophorbide a May Regulate Jasmonate Signaling during Dark-Induced Senescence, Plant Physiol., 182 (2020) 776-791.
[29] S. Moser, T. Erhart, S. Neuhauser, B. Kräutler, Phyllobilins from senescence associated chlorophyll breakdown in leaves of basil (Ocimum basilicum) show increased abundance upon herbivore attack, J. Agric. Food Chem., (2020).
[30] V. Buchanan-Wollaston, T. Page, E. Harrison, E. Breeze, P.O. Lim, H.G. Nam, J.F. Lin, S.H. Wu, J. Swidzinski, K. Ishizaki, C.J. Leaver, Comparative transcriptome analysis reveals significant differences in gene expression and signalling pathways between developmental and dark/starvation-induced senescence in Arabidopsis, Plant J., 42 (2005) 567-585.

Fig. 1

A

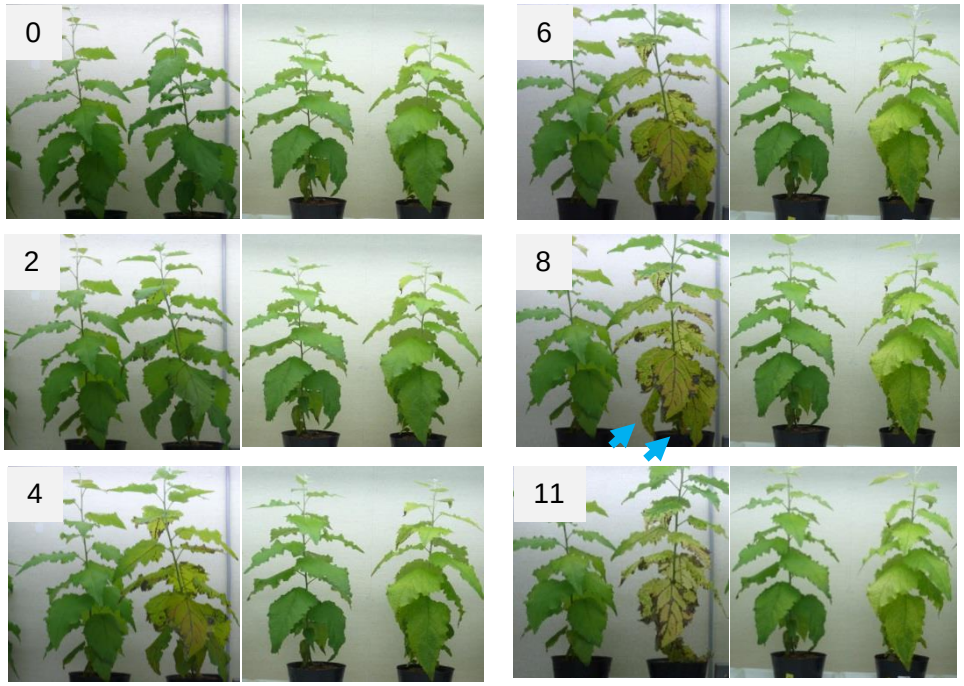
0
6
2
8
4
11
mock DEX
Line 1
mock DEX
Line 2
mock DEX
Line 1
mock DEX
Line 2

B

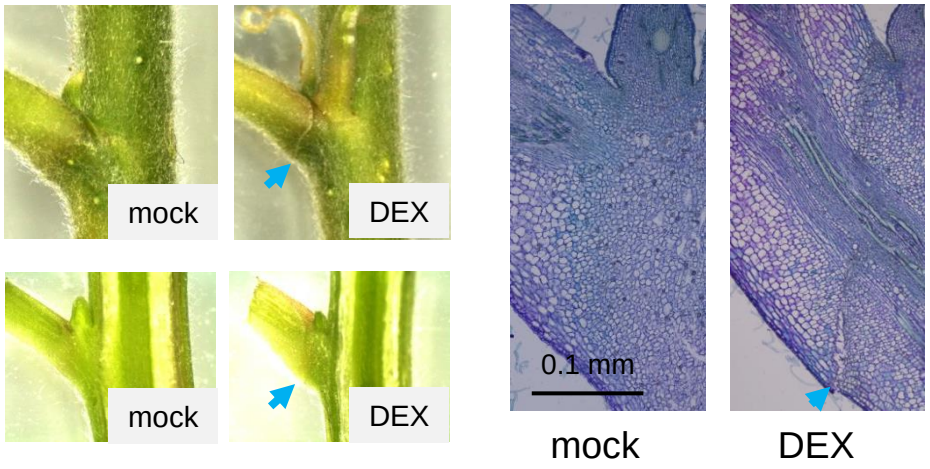
mock
DEX
mock
DEX
0.1 mm
mock
DEX

Fig. 2

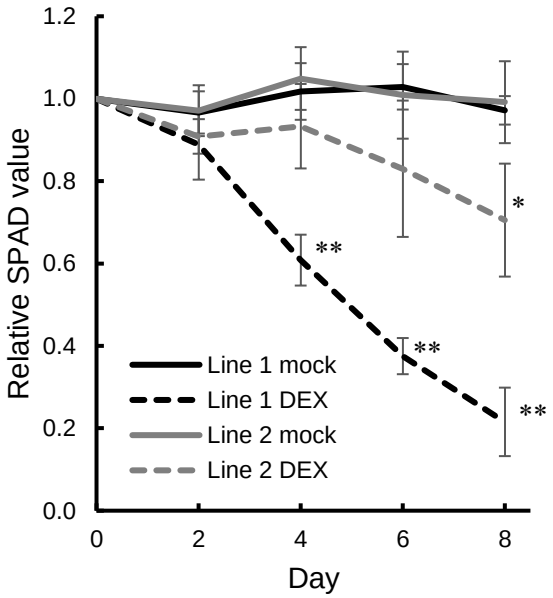
1.2
1.0
0.8
0.6
0.4
0.2
0.0
Relative SPAD value
0
2
4
6
8
Day
Line 1 mock
Line 1 DEX
Line 2 mock
Line 2 DEX
*
**
**
**

Fig. 3

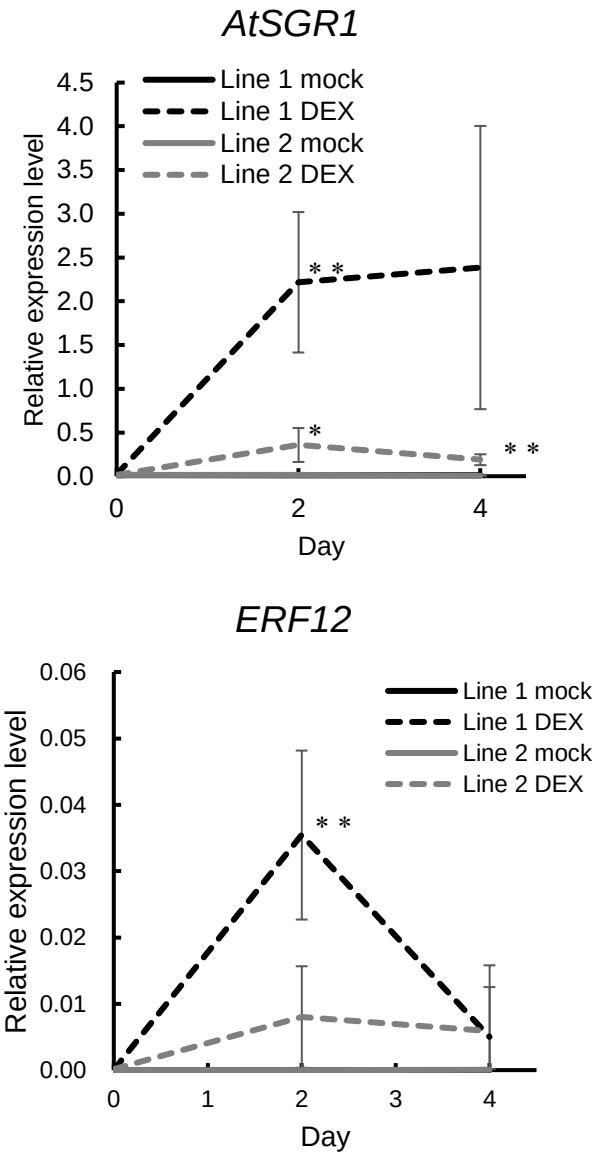
AtSGR1
Line 1 mock
Line 1 DEX
Line 2 mock
Line 2 DEX
Relative expression level
4.5
4.0
3.5
3.0
2.5
2.0
1.5
1.0
0.5
0.0
* *
*
* *
0
2
4
Day
ERF12
Line 1 mock
Line 1 DEX
Line 2 mock
Line 2 DEX
Relative expression level
0.06
0.05
0.04
0.03
0.02
0.01
0.00
* *
0
1
2
3
4
Day

Fig. 4

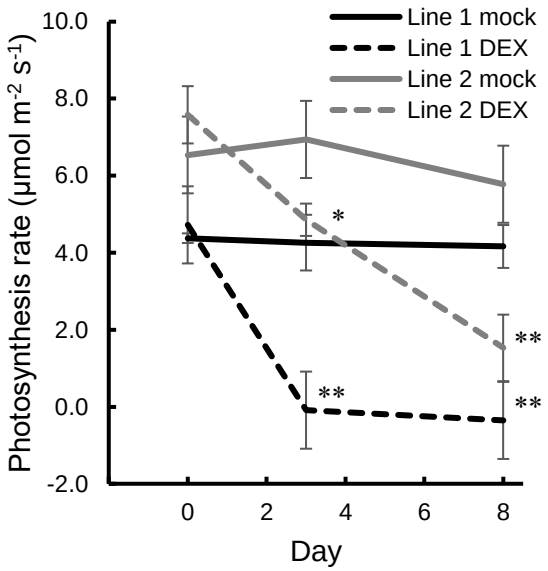
Line 1 mock
Line 1 DEX
Line 2 mock
Line 2 DEX
Photosynthesis rate (μmol m-2 s-1)
10.0
8.0
6.0
4.0
2.0
0.0
-2.0
0
2
4
6
8
Day
*
**
**
**

Fig. 5

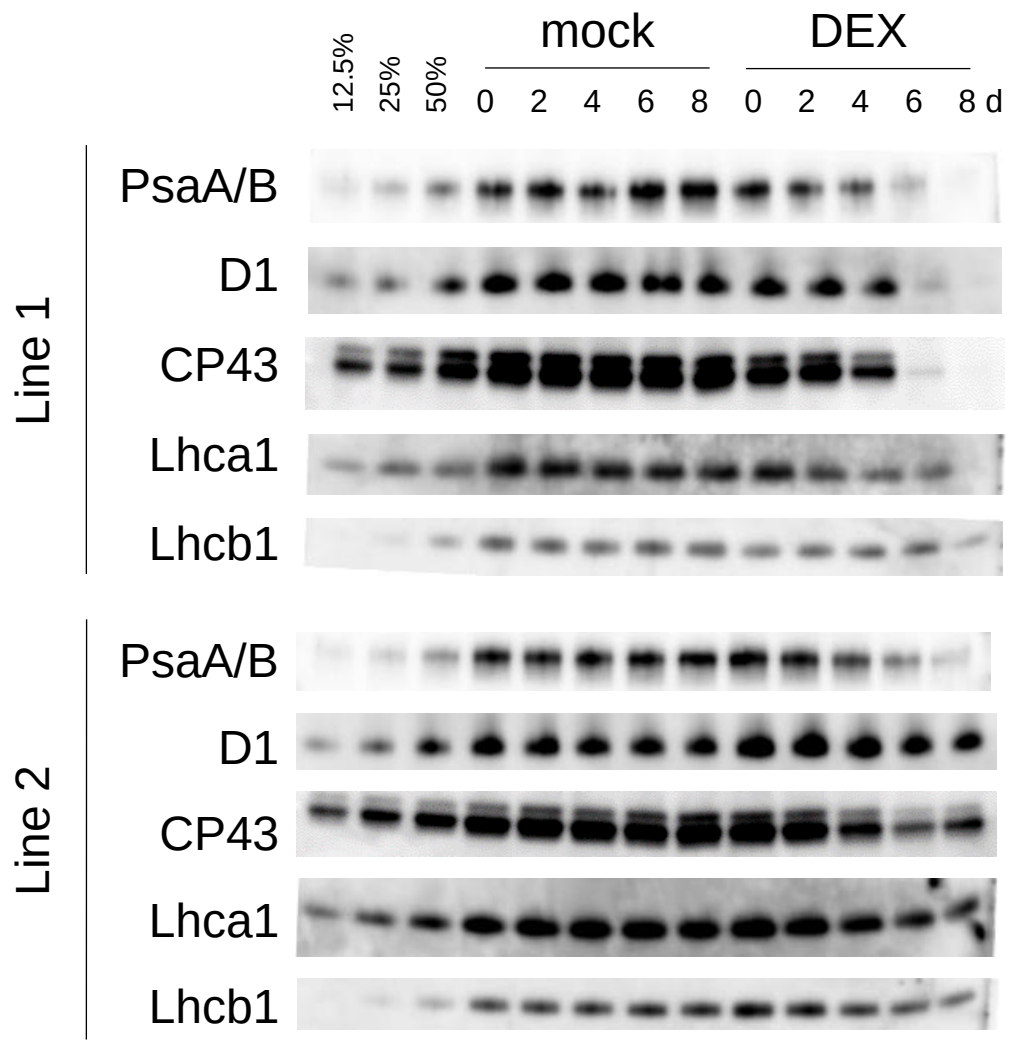
12.5%
25%
50%
mock
DEX
0 2 4 6 8 0 2 4 6 8 d
Line 1
PsaA/B
D1
CP43
Lhca1
Lhcb1
Line 2
PsaA/B
D1
CP43
Lhca1
Lhcb1

Fig. 6